

Engineering molecular aggregate spectra

V. A. Malyshev¹, A. V. Malyshev^{1,2,*}

¹ Centre for Theoretical Physics and Zernike Institute for Advanced Materials, Nijenborgh 4, 9747 AG Groningen, The Netherlands

² Ioffe Physical Technical Institute, 194021 Saint-Petersburg, Russia

Received XXXX, revised XXXX, accepted XXXX

Published online XXXX

PACS 42.70.-a 67.30.ht 68.47.Pe 73.20.Mf 74.25.Jb 8107.-b

* Corresponding author: e-mail a.malyshev@rug.nl, Phone +31-50-3634784, Fax +31-50-3634754

We show that optical properties of linear molecular aggregates undergo drastic changes when aggregates are deposited on a metal surface. The dipole-dipole interactions of monomers with their images can result in strong re-structuring of both the exciton band and the absorption spectrum, depending on the arrangement of the monomer transition dipoles with respect to the surface.

Copyright line will be provided by the publisher

1 Introduction Molecular aggregates, in spite of more than 70 years of history after their discovery by Jelley [1] and Scheibe [2], still attract a great deal of attention due to their extraordinary optical and transport properties: narrow absorption band, superradiant emission, giant higher order susceptibilities and light harvesting [3,4]. Nowadays, the problem of controlling the optical properties of molecular aggregates is a challenging task.

In an isolated aggregate, the energy of optical transition is determined by the transition energy of a monomer, which is fixed for a particular monomer, as well as by the transfer (dipolar) interactions, which are also fixed by the aggregate morphology. Therefore, there is almost no way to influence the optical absorption for a single aggregate. Being embedded into a host, an aggregate interacts with it, which results in the so-called “solvent” shift of its absorption line. Difference in local solvent environment gives rise to an inhomogeneously broadened absorption band. Coupling of aggregates to vibrational degrees of freedom leads to homogeneous broadening of the aggregate absorption band. In different hosts, both the position of the aggregate absorption peak and its width vary to some extent. However, both effects are usually not very pronounced (see, e.g., Ref. [5]).

As it has been pointed out in a number of papers, the optical response of J-aggregates changes substantially when J-aggregates are deposited on colloidal noble metal nanoparticles. Thus, super-radiant lasing at low threshold [6] and re-structuring of the absorption spectra [7,8,9,10]) have

been reported. We consider aggregates deposited on a flat metallic surface and show that the aggregate absorption spectrum experiences strong modifications: the bare absorption band shifts and new bands also arise. The effect originates from the interaction of monomer transition dipoles with their images in the metal. As a result, a simple linear aggregate converts into an effective double-strand structure. The changes in the absorption spectrum are sensitive to the arrangement of the transition dipoles with respect to the metal surface.

Throughout the paper, we restrict ourselves to the case of molecular J-aggregates. An analogous study for the other type of aggregates, the so-called H-aggregates deposited on a metal surface, which is also an interesting example, will be published elsewhere.

2 Modeling aggregates

2.1 A stand-alone aggregate We model a single aggregate as an open linear chain of N optically active two-level units (monomers) with parallel transition dipoles coupled to each other by dipole-dipole transfer interactions which delocalize the excitation. Because of that coupling, optical excitations of the chain are Frenkel excitons described by the Hamiltonian

$$H_{\text{ex}} = \sum_{n=1}^N \epsilon_n |n\rangle \langle n| + \sum_{n,m} J_{nm} |n\rangle \langle m|, \quad (1)$$

Copyright line will be provided by the publisher

where $|n\rangle$ denotes the state in which only n th monomer is excited and ϵ_n is its excitation energy. These energies are uncorrelated and taken at random from a box distribution with the mean ϵ_0 (the excitation energy of an isolated monomer which we set to zero from now on) and the standard deviation σ . The dipolar transfer interactions $J_{nm} = J/|n - m|^3$ ($J_{nn} \equiv 0$) are considered to be non fluctuating. The parameter $J = (\mathbf{d}^2/a^3)(1 - 3\cos^2\theta)$ represents the nearest-neighbor transfer interaction, \mathbf{d} being the transition dipole moment of a monomer tilted at an angle θ with respect to the aggregate axis and a being the nearest-neighbor distance. A negative sign of the couplings J_{nm} corresponds to the case of J-aggregates. The exciton energies ϵ_ν ($\nu = 1, \dots, N$) and wavefunctions $\varphi_{\nu n}$ (taken to be real) are obtained after diagonalization of the $N \times N$ Hamiltonian matrix $\langle n|H_{\text{ex}}|m\rangle$.

2.1.1 A single aggregate deposited on a metallic surface We address an aggregate deposited on a conductor surface within the framework of the image potential approximation, the simplest way to account for the presence of the metal (see Fig. 1). The applicability of the method in the present case can be rationalized as follows. First, the typical frequency of plasmon oscillations in a good conductor is on the order of 10^{16}s^{-1} , whereas the optical transition frequency in J-aggregates is about an order of magnitude smaller. Furthermore, the electron relaxation in metals is much faster than the exciton optical dynamics. Typical electron relaxation time is $10 \div 100$ fs (see, e.g., Ref. [11]), while the characteristic optical dynamics time in the prototype J-aggregates of the pseudoisocyanine dye is $10 \div 100$ ps (see, e.g., Refs. [12, 13]). Therefore, conduction electrons represent a fast system instantly following all charge redistributions in the aggregate at the exciton related time scale.

It is worthwhile to note also that, contrary to the present case of a *bulk* metallic substrate, the image potential method can usually not be justified for a J-aggregate adsorbed onto a metal *nano-particle*. In the latter case, the frequency of surface plasmons in the particle is often on the order of the optical frequency, therefore strong mixing of excitons and plasmons should be taken into account (see discussions in Refs. [14] and [15]).

Within the framework of the image approximation, the total Hamiltonian $H = H_{\text{ex}} + H_{\text{img}} + H_{\text{ex-img}}$ consists of the Hamiltonian of the aggregate H_{ex} , Eq. (1), that of the image dipoles H_{img} and the Hamiltonian $H_{\text{ex-img}}$ which describes the interaction of the aggregate monomers with all images in the metal. It is straightforward to write out explicit expressions for H_{img} and $H_{\text{ex-img}}$. We note that (i) the image Hamiltonian in the cite representation is diagonal with image transition energies equal to those of the corresponding monomers, and that (ii) image dipoles do not interact with each other. The latter can be understood in the following way. A charge near a metal surface gives rise to the redistribution of charges on the surface, which is equivalent to introducing an image charge. The surface

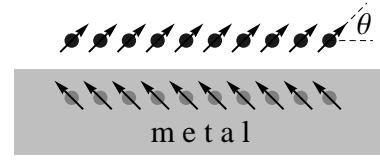


Figure 1 Cartoon of an aggregate deposited on a metal surface. The monomer transition dipoles (black circles with arrows) induce their images in the metal (gray circles with arrows). An image is formed in such a way that the component of the transition dipole perpendicular to the metal surface is conserved, while the one along the surface is inverted. Real transition dipoles interact with all images while images do not interact with each other (see the discussion in the text).

charge distribution created by two charges is a sheer linear combination of the two distributions induced by the charges independently (because of the superposition principle). Should there be an interaction between the corresponding images, the overall potential would have an additional part due to the interaction, which is not the case. However, the interaction of images with the external electromagnetic field should be taken into account. The following comment is due here: consider radiation field of a dipole emitter near a metal surface; the field of the system in the far zone would contain the contribution from the dipole and the one from the induced surface charge distribution, the latter being equivalent to the field of the image. The system would emit therefore as a quadrupole, suggesting that we should treat it as a system of two real dipoles in this case. The same applies to the excitation of the system by an external field.

The new exciton energies and wavefunctions can be obtained after diagonalization of the $2N \times 2N$ Hamilton matrix $\langle n|H|m\rangle$, similar to the case of the stand-alone aggregate.

3 Results and discussion We calculated the density of states (DOS) and the absorption spectrum defined, respectively, as

$$\text{DOS}(E) = \frac{1}{2N} \left\langle \sum_{\nu=1}^{2N} \delta(E - \epsilon_\nu) \right\rangle \quad (2)$$

$$A(E) = \frac{1}{2N} \left\langle \sum_{\nu=1}^{2N} \left(\sum_{n=1}^{2N} \varphi_{\nu n} \right)^2 \delta(E - \epsilon_\nu) \right\rangle, \quad (3)$$

where the angular brackets denote the average over disorder realizations. In the simulations, aggregates of $N = 300$ monomers were considered. For aggregates deposited on a metal surface, we assumed the transition dipole moments of monomers \mathbf{d} lying in the plane perpendicular to the metal surface.

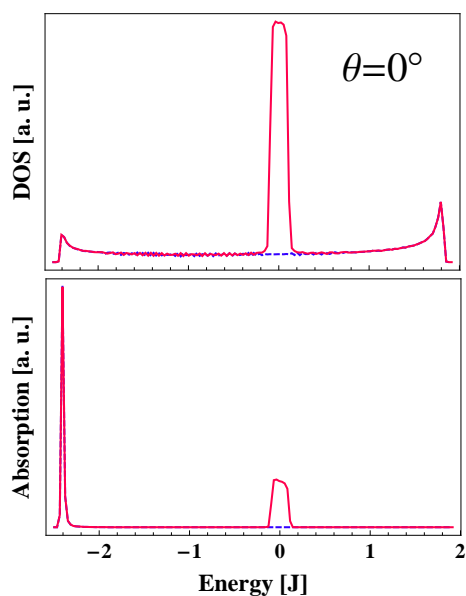


Figure 2 DOS (upper panel) and absorption spectra (lower panel) of aggregates in a glassy host (dashed curves) and deposited on a metallic surface (solid curves). The set of parameters used in simulations is: the disorder strength $\sigma = 0.2J$, the angle between the monomer transition dipole and the surface $\theta = 0$, and the distance between aggregates and the surface $d = a$.

In Figs. 2 and 3 we show the results of our simulations of the DOS (upper panel) and the absorption spectra (lower panel) for $\sigma = 0.2J$. The dashed curves represent the data obtained for stand-alone aggregates in a glassy host (in the absence of the metal). The solid curves show the same quantities calculated for aggregates deposited on the surface of a metal with the aggregate-surface separation $d = a$, so that the distance between a monomer and its image is equal to $2a$. The data presented in Figs. 2 and 3 were obtained for the tilting angles $\theta = 0$ and $\theta = \pi/4$, respectively.

In the absence of the metal, the DOS and the absorption spectra exhibit standard shapes: the DOS reveals two singularities at the band edges (smoothed by the disorder) while the absorption has a peak at the lower band edge (the J-band). The picture changes dramatically for deposited J-aggregates. Along with the band edge singularities of the DOS, very pronounced features arise at the center of the band for both tilting angles (upper panels in Figs. 2 and 3). The DOS reconstruction is accompanied by the occurrence of an additional intense line at the band center (about the monomer energy). For the tilting angle $\theta = \pi/4$ the bare J-band shifts to the red, reflecting the corresponding shift of the lower energy band edge.

The changes that occur in the DOS and the absorption spectra of deposited aggregates can be qualitatively

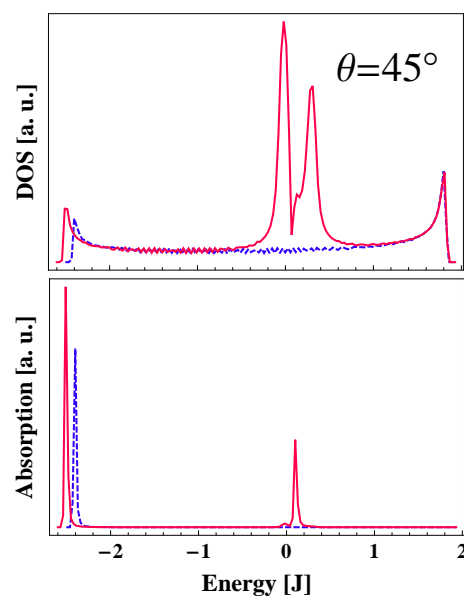


Figure 3 Same as in Fig. 2 calculated for $\theta = \pi/4$.

understood within a simplified model which takes into account the coupling of a monomer to its own image only, neglecting couplings to images of other monomers. A deposited aggregate can then be viewed as a system of dimers (monomer-image) coupled to each other via the monomer-monomer transfer interactions J_{nm} . For $d = a$ and $\theta = 0$, the magnitude of coupling between neighboring monomers, $|J| = 2|d|^2/a^3$, is 16 times larger than that between a monomer and its image, $|d|^2/8a^3$. In this case the images can be considered to be almost decoupled from the monomers, which gives rise to δ -peaks in the DOS at monomer energies ε_n . The image states would have the monomer oscillator strength, resulting in the appearance of the new absorption band about the monomer energy (see Fig. 2). The lineshape of the new band reproduces the distribution function of the on-site energies. In the vicinity of the “magic” angle $\theta = \arccos(1/\sqrt{3}) \approx 57^\circ$, at which the monomer-monomer transfer interactions J_{nm} vanish, the system can be viewed as a set of weakly coupled dimers. The two eigenstates of a dimer would then give rise to their own bands due to weak coupling to neighbors. This trend can be seen in the Fig. 3 where the appearance of band edge singularities in the DOS is clearly visible. The singularities give rise to additional features in the absorption. A more comprehensive study of the optical properties of deposited molecular aggregates will be published elsewhere.

4 Summary and concluding remarks We studied numerically the absorption spectra of J-aggregates deposited on a surface of a metal. We found that the density of states and the absorption spectra undergo strong changes which depend on the arrangement of the monomer transi-

tion dipoles with respect to the metal surface. In particular, within some range of the transition dipole tilting angle, the original J-band shifts to the red and a new intense absorption band appears in the middle of the exciton band (about the monomer energy). Our findings open a new perspective for designing optical properties of molecular aggregates.

Acknowledgements A. V. M. acknowledges support from NanoNed, a national nanotechnology program coordinated by the Dutch Ministry of Economic Affairs.

References

- [1] E. E. Jelley, *Nature* **139**, 631 (1936).
- [2] G. Scheibe, *Angew. Chem.* **50**, 212 (1937).
- [3] T. Kobayashi (ed.), *J-aggregates* (World Scientific: Singapore, 1996).
- [4] J. Knoester, in *Proceedings of the International School of Physics "Enrico Fermi"*, Course CXLIX, edited by V. M. Agranovich and G. C. La Rocca (IOS Press, Amsterdam, 2002), p. 149.
- [5] I. Renge and U. P. Wild, *J. Chem. Phys. A* **101**, 7977 (1997).
- [6] S. Özçelik and D. L. Akins, *Appl. Phys. Lett.* **71**, 3057 (1997); S. Özçelik, I. Özçelik, and D. L. Akins, *Appl. Phys. Lett.* **73**, 1949 (1998).
- [7] N. Kometani, M. Tsubonishi, T. Fujita, K. Asami, and Y. Yonezawa, *Langmuir* **17**, 578 (2001).
- [8] G. A. Wurtz, and J. E. Hranisavljevic, *Nano Lett.* **4**, 2121 (2004).
- [9] T. Uwada, R. Toyota, H. Masuhara, T. Asahi, *J. Phys. Chem. C* **111**, 1549 (2007).
- [10] A. M. Kelley, *Nano Lett.* **7**, 3235 (2007).
- [11] *Handbook of Optical Constants of Solids*, edited by E. D. Palik; Academic: San Diego, 1985.
- [12] H. Fidder, J. Knoester, and D. A. Wiersma, *Chem. Phys. Lett.* **171**, 529 (1990).
- [13] D. J. Heijs, V. A. Malyshev, and J. Knoester, *Phys. Rev. Lett.* **95**, 177402 (2005); *J. Chem. Phys.* **123**, 144507 (2005).
- [14] I. A. Larkin, M. I. Stockman, M. C. Achermann, and V. I. Klimov, *Phys. Rev. B* **69**, 121403(R) (2004).
- [15] V. A. Markel, *Phys. Rev. E* **72**, 023401 (2005); *Phys. Rev. B* **74**, 216401 (2006).